RECENT ADVANCES IN THE RETRIEVAL OF METEOROLOGICAL PARAMETERS THROUGH THE "3I" SYSTEM

N. A. Scott, A. Chedin, F. M. Breon, C. Claud,
J. F. Flobert, N. Husson, C. Levy, and Y. Tahani

Laboratoire de Meteorologie Dynamique du CNRS
Ecole Polytechnique, 91128 Palaiseau Cedex, France

G. J. Prangsma

Koninklijk Nederlands Meteorologisch Instituut
P.O. Box 201, 3730 AE De Bilt, Netherlands

G. Rochard

EERM, Centre de Meteorologie Spatiale
P.O. Box 147, 22302 Lannion Cedex, France

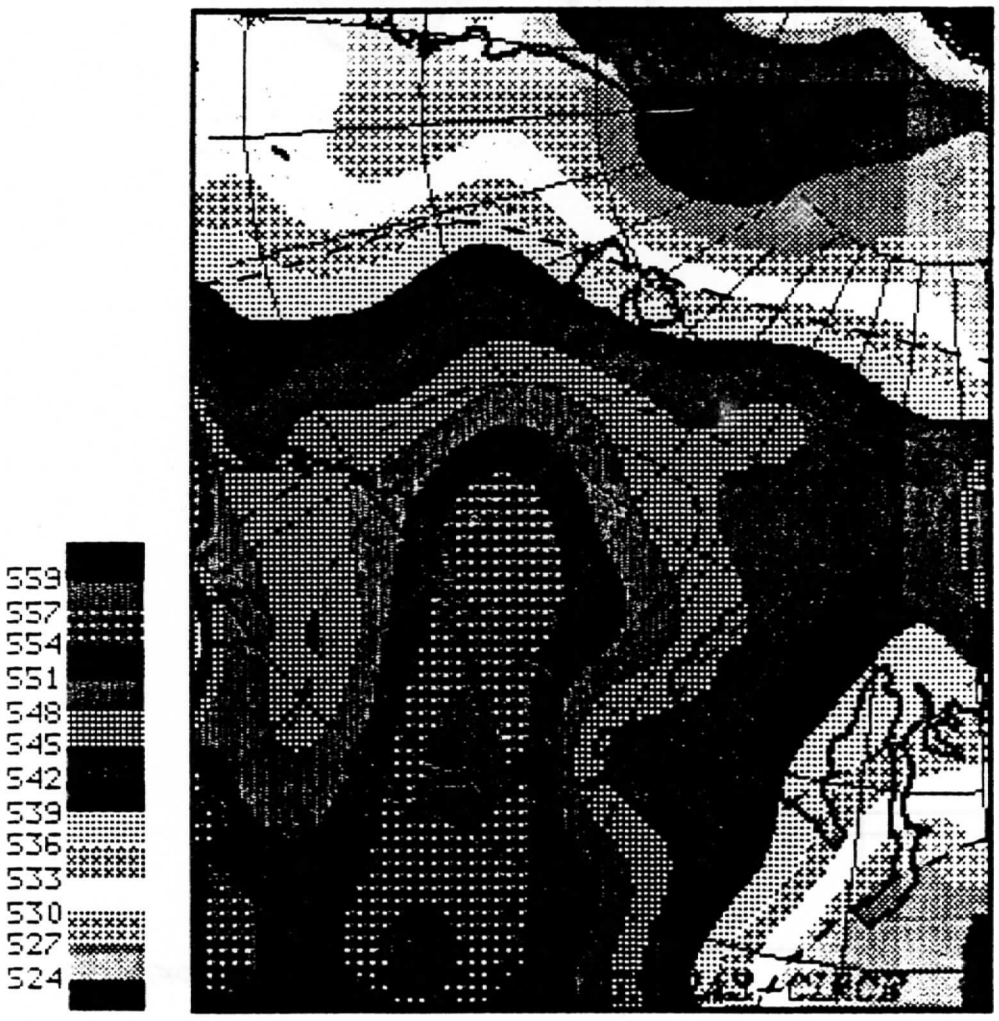

March 1988

Cover Figure: 3I retrieved geopotential thicknesses for the layer 1000-500 hPa, NOAA-9, 5 June 1986 at 9.57Z. ARCTEMIZ CAMPAIGN. Superimposed: ECMWF analysis for the same day at 12.00Z. Values range from 524 dam (blue) to 559 dam (red).

1. INTRODUCTION

Aiming at the three-dimensional analysis of the Earth's atmosphere structure from observations of the operational meteorological satellites of the TIROS-N/NOAA series, algorithm "3I", since the last meeting of the International TOVS working group, has been developed and refined following three main directions :

- improvement of the physics involved for a better handling of a priori information on the medium observed in the pattern recognition approach to initialization of the inversion process leading to a better accuracy of the retrieved products. In particular, the role of the surface, the detection and impact of snow and ice, the role of the clouds in the water vapor inversion, have been the subject of detailed studies ;

- through numerous applications to special situations, 3I has progressively been extended and now produces retrievals at global scale. These applications were conducted either within international programmes : MIZEX and ARCTEMIZ for polar latitudes, FASINEX and GALE for west Atlantic at low latitudes, or through cooperations with meteorological offices : France (CMS, Lannion), Netherlands (KNMI, De Bilt), China (CMS, Beijing), Europe (ECMWF, Reading), etc... ;

- improvement and simplification of the code itself for a more rational use in routine or in operation and for an easier transfer to other centers. In particular, the "educated" data set "TIGR" (TOVS Initial Guess Retrieval) has been made unique, whatever the number of satellites to be processed is. Its validation, from one satellite to a new one has been greatly simplified and can now be easily done by any center.

2. DETERMINATION OF MESOSCALE METEOROLOGICAL PARAMETERS FOR POLAR LATITUDES

2.1 Introduction

Observations from the satellites of the TIROS-N series on polar regions, where in-situ data are very scarce are helpful for the study of the interactions between ocean, ice and atmosphere through the retrieval of atmospheric and surface parameters. The "3I" - Improved Initialization Inversion - method (Chedin et al., 1985 ; Chedin and Scott, 1986), developed in the past few years at LMD, has shown ability to retrieve with a good accuracy temperature profiles through inversion of the Radiative Transfer Equation (Le Marshall, 1985). The MIZEX (Marginal Ice Zone EXperiment) and ARCTEMIZ (MIZ of the European ARCTic) campaigns, conducted respectively during the summer 1984 in the Fram Strait and since 1986 north and south of Fram Strait, have given the opportunity of applying this retrieval algorithm to high latitude observations. Associated to numerous in situ data, these campaigns have also allowed for comparisons with the retrieved products.

Satellite data have been provided by the Tromso Telemetry Station (Norway). TOVS data were on HRPT format tapes associated with corresponding images from AVHRR channel 2 ; the TOVS data have been navigated and calibrated at the Centre de Météorologie Spatiale in Lannion (France). MSU data are corrected for limb effects, liquid water attenuation and surface effects with the exception of MSU1 which is not corrected for surface effects.

In situ data include radiosoundings acquired during the campaigns and coming either from ships or from the synoptic network. For MIZEX, they have been obtained from the World Data Center for Glaciology, Boulder, USA. In addition, synoptic maps, ice charts and sea surface temperature analyses for the period of the campaign are also available (Lindsay, 1985). For the ARCTEMIZ campaign, surface analyses and thicknesses charts have been obtained from the SMHI and the ECMWF.

Five days for MIZEX (5th and 19th of June 1984, 1st and 2nd of July 1984, 5th of August 1984) and 17 consecutive days for ARCTEMIZ (from 5th to 21st of June 1986) have been processed through the inversion algorithm "3I" and results have been compared with conventional data.

2.2 Detection of sea ice. Incidence on the cloud detection procedure

Discriminating between the elements of a system comprising open water, sea ice and cloud from space observations is a well identified problem : for a clear situation and day time observations, distinction between sea ice and open water is a relatively easy task since their albedo (obtained from the visible channel) is very different. Obviously, this approach cannot be used for cloudy conditions or night time observations. Microwave observations due to their low sensitivity to clouds may help the solution to the problem in most cases. Moreover, microwave observations display an interesting property related to the variation of emissivity (ϵ) at 50 GHz with the type of the surface : sea ice, from young (ϵ = 0.95) to multiyear (ϵ = 0.7) and open water (ϵ = 0.6).

Two different methods for determining surface emissivities directly from satellite observations have been developed and are briefly described below.

Direct statistical method

This method relies upon the fact that channel MSU1 is sensitive to surface emissivity and to temperature in the lower atmosphere and down to the surface whereas channel MSU2 is mostly a function of the temperature of the low atmosphere and relatively not sensitive to the surface because of its low overall transmission (close to 0.1). It is thus possible to extract the surface emissivity from a combination of these 2 channels. Such a particularity has already been used by Grody (1983).

A relation between the surface emissivity ϵ, the brightness temperature of MSU channel 1, TBMSU1, and MSU channel 2, TBMSU2, has been established under a form similar to the one found by Grody :

$$\epsilon = a + b\ TBMSU1 + c\ TBMSU2$$

In Grody's approach, the coefficients have been obtained from a sample of data restricted in space (United States) and in time (April 1979).

In our study, the coefficients a, b, c have been regressed independently for the polar situations and for the mid-latitude situations archived in TIGR. There are 525 polar type situations and 545 mid-latitude situations in TIGR (cf. Table 1).

Latitude class	Number of situations	a	b	c	Standard deviation on ϵ
Polar	525	0.797	0.0082	-0.0083	0.040
Midlatitude	545	1.080	0.0074	-0.0083	0.032

Table 1 Values of the different constants a, b, c, for the two latitude zones concerned.

Direct physical method

Microwave surface emissivity may also be extracted by considering the Radiative Transfer Equation itself. The measured radiance can be written as follows :

$$I = \epsilon\ [\tau B_s - \tau \int^{\downarrow} B d\tau] + [\int^{\uparrow} B d\tau + \tau \int^{\downarrow} B d\tau]$$

For a given class (polar or mid latitude), it has been found that the quantities τ, $\int\uparrow B d\tau$ and $\int\downarrow B d\tau$ may be considered as constant to within a good approximation, at least with the purpose of determining ϵ to the

required accuracy. Standard deviations of each of these quantities and their means are given in Table 2.

As a consequence and using the Rayleigh Jeans approximation (radiance is a linear function of temperature), the preceding equation may be written as :

$$TBMSU1 = \epsilon \, [\tau \, T_s - \alpha] + \beta$$

This relation indicates that emissivity may be obtained when MSU1 brightness temperature and surface temperature are known.

Transmittance values are calculated using the fast line-by-line model"4A" (N.A. Scott, A. Chedin, 1981) and the surface temperature can be estimated from HIRS-2 channel 8 brightness temperature corrected for water vapour and surface emissivity effects (Wahiche, 1984).

	Midlatitude		Polar latitude	
	Mean value	Standard deviation	Mean value	Standard deviation
τ	0.679	0.012	0.664	0.012
$\int \uparrow B d\tau$	$1.89\ 10^{-3}$	$0.02\ 10^{-3}$	$1.90\ 10^{-3}$	$0.02\ 10^{-3}$
$\int \downarrow B d\tau$	$1.97\ 10^{-3}$	$0.03\ 10^{-3}$	$1.97\ 10^{-3}$	$0.03\ 10^{-3}$

Table 2 Mean values and standard deviations for the quantities τ, $\int \uparrow B d\tau$ and $\int \downarrow B d\tau$ for the 545 midlatitude situations and the 525 polar situations archived in TIGR. $\int \uparrow B d\tau$ and $\int \downarrow B d\tau$ are expressed in $mw.cm^{-2}.sr^{-1}$.

Using results of Table 2, we may write TBMSU1 as follows :

$TBMSU1 = \epsilon \, (0.664 \, T_s - 56.24) + 137.9$ Polar zone

$TBMSU1 = \epsilon \, (0.679 \, T_s - 57.42) + 138.8$ Midlatitude zone

In the recent past, another attempt has been made to detect and delimit sea ice using MSU data (Yamamouchi, Seo, 1984). Instead of using a threshold value for the emissivity, their method is based on a threshold value on the MSU1 brightness temperature. We have applied their method to the satellite observations considered in this study. The results are not always satisfactory. This is apparently due to T_s which is considered as a constant whereas it shows an important variability.

Results and discussion

For each of the selected orbits, surface microwave emissivities have been calculated by the two direct methods described above. Results are very similar apart from a systematic bias of about 0.1 (larger values for the physical method). However, such a bias does not prevent either method from identifying sea ice covered areas. The mean of the values given by these two methods is very close to the value obtained through the full physical inversion method (Wahiche, 1984). Results are illustrated on Figure 1 for a NOAA-9 pass on June 11, 1986. Sea ice is displayed in red and pink. Results too close to coast lines should be discarded due to the low resolution of the MSU sounder.

Impact of this information on cloud detection

Two tests, which are also part of the operational NOAA/NESDIS retrieval algorithm (McMillin et al., 1982) may benefit from an a priori knowledge of the presence of sea ice : the so-called "frozen sea" test and the albedo test. Details on the modifications introduced as well as more details on the methods reported here are given in Claud et al. (1988). Results are illustrated on Figure 2 for the same pass as above.

2.3 Geopotential thicknesses

As an example of the results obtained for the domain observed, the cover plate shows for a particular pass (5 June 1986, 9:57Z) retrieved geopotential thicknesses for the layer 1000-500 mb (in dam).

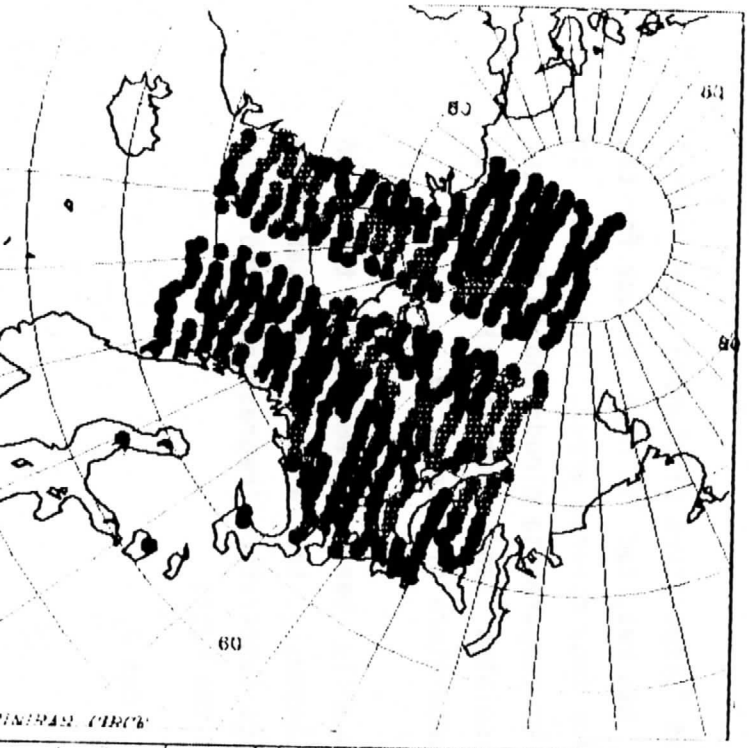

Figure 1

Microwave surface emissivity. NOAA-9. 11 June 1986. ARCTEMIZ campaign. Sea ice is in red and pink. Results close to coast lines should be discarded as contaminated by the continent.

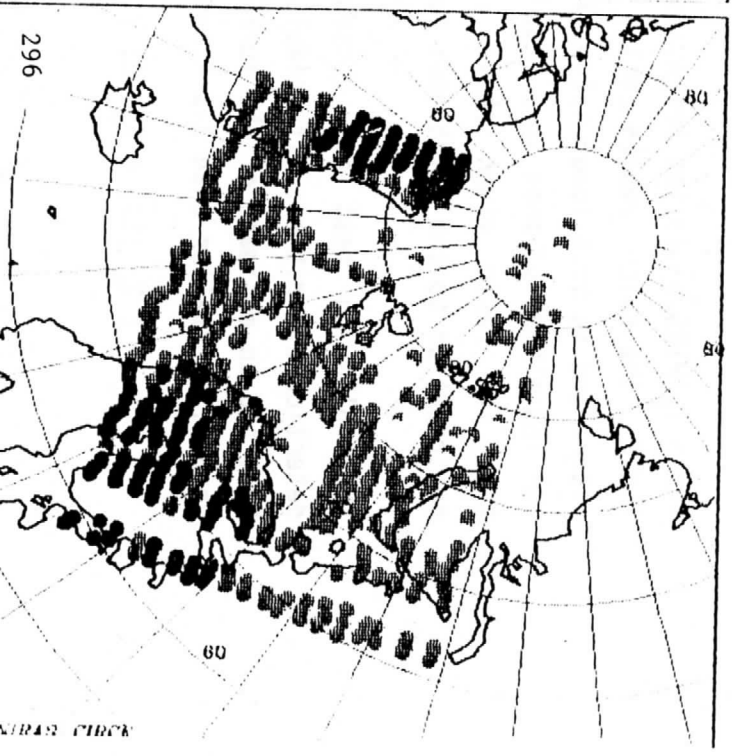

Figure 2

Results of the revised cloud detection algorithm. In blue (over sea) and green (over land) are the clear areas. The cloud system between Svalbard and Norway was not detected previously.

Figure 3 Snow detection from HIRS-2. Snow : yellow. Clear areas : blue (sea) or green (land). NOAA-9. Orbit 6209.

Comparisons with analyses coming from either the ECMWF or the SMHI for the same day at 12:00Z, show good agreement. "3I" retrieved maps display more details : see for example the warm air coming from the Scandinavian continent and going in two directions (towards Greenland and towards Franz Joseph Land). Analyses indicate only one axe (towards Franz Joseph Land).

This work is developing towards analysis of situations characterized by "polar lows", in cooperation with DNMI (Norvegian Meteorological Institute).

3. DETECTION OF SNOW FROM HIRS-2

Because of its high albedo, snow cover is often seen as cloud by cloud detection algorithms during day time. Moreover, snow and low cloud top temperatures may be similar. It has already been reported in the literature (see for example : S.Q. Kiddder et al., Mon. Wea. Rev., 112, 2345) that comparisons between channels at 11μm and 3.7 μm could help discriminating between snow and clouds. Computation of the ratio :

$$\{ T_B \text{ (HIRS,19)} - T_B \text{ (HIRS,8)} \} / \cos \theta_s ,$$

where T_B(HIRS,n) is the brightness temperature of channel n of HIRS-2 and θ_s the solar zenith angle, has resulted in high values for the clouds and in much lower values for snow covered areas. This is due to the low albedo of snow at 3.7 μm as compared to clouds and to the fact that the ratio given above isolates (and normalizes) the solar contribution to the brightness temperature of channel 19.

The following test has consequently been implemented in the cloud detection algorithm : if, simultaneously, the albedo is greater than 20%, and an estimate of the surface temperature (regression based upon channel 8) smaller than 273 K and the ratio

$$\{ T_B \text{ (19)} - T_B \text{ (8)} \} / \cos \theta_s$$

smaller than 14 K, the field of view considered is supposed to be clear, with snow covering it. Several NOAA-9 passes have been processed, for which manual nephanalyses had clearly identified snow covered areas. Figure 3 illustrates one example. Snow in in yellow and the areas concerned are in perfect agreement with manual analysis.

4. ANALYSIS OF SATELLITE OBSERVATIONS OVER WEST ATLANTIC : FASINEX AND GALE EXPERIMENTS

4.1 Introduction

During February 1986, the FASINEX experiment was in its intensive phase. It was designed to study the response of the upper ocean to atmospheric forcing, the response of the atmosphere in the vicinity to an oceanic front, and the associated two way interaction between ocean and atmosphere. For this experiment, there was one research ship on each side of a very sharp oceanic front, launching radiosondes every 6 hours and studying the ocean in the vicinity of the front (SST, fluxes, velocity profiles). Data from satellites, aircrafts and buoys were also collected (Stage and Weller, Bull. Amer. Meteor. Soc., 67, 1986).

During the same period of February 1986, the GALE experiment (Genesis of Atlantic Lows Experiment) went on over the same area, on a somewhat larger scale. This experiment intended to study the atmospheric cyclogenesis over the American East coast. February 24th was seen as the biggest cyclogenesis day.

The California Space Institute (CSI) is deeply involved in the FASINEX experiment and has archived the corresponding data. The interest of studying, for both FASINEX and GALE, the atmospheric signal shown by satellite data using 3I retrieval method, has led CSI and our group to start cooperating (Drs. C. Gautier and J. Bates).

4.2 Implementation of the 3I system on CSI VAX computer

The 3I system has been implemented on a micro-VAX I at CSI, starting from the version installed at CIRCE (Centre Inter-Régional de Calcul Electronique), France (IBM-3090 and Siemens VP200 computers). Table 3 shows the computer resources needed for this method (retrieval procedure from calibrated, navigated satellite data, to atmospheric parameters). These results and especially the 1h15mn elapsed time for a one orbit retrieval (about 130 HIRS scan lines), shows that the 3I system can be used easily on an operational daily basis with a micro-VAX computer connected to an HRPT receiving station.

Charged CPU	1 h 00 mn
Central Memory	3 MBytes
Elapsed Time	1 h 15 mn
TIGR Size	35 MBytes
Topography File (global)	16 MBytes

Table 3 Computer needs for the "3I" retrieval method running on a Micro-VAX

4.3 The results

At CSI, TOVS data have been analysed using 3I for 16 NOAA-9 passes from February to mid-March. The physical parameters retrieved by 3I over the area covered by the satellite passes are : air mass types (polar, temperate or tropical), temperature profiles, geopotential thicknesses, thermal winds, cloud heights, cloud amounts (equivalent of black clouds), surface emissivity, total water-vapor content and three layers relative humidities. About 150 radiosoundings have been collocated with retrievals. AT LMD, 5 passes (out of the 16) have been processed and 3 of them, around the period of the most active cyclogenesis (February 24th and 25th) in great detail. Figures 4 and 5 present, for seven

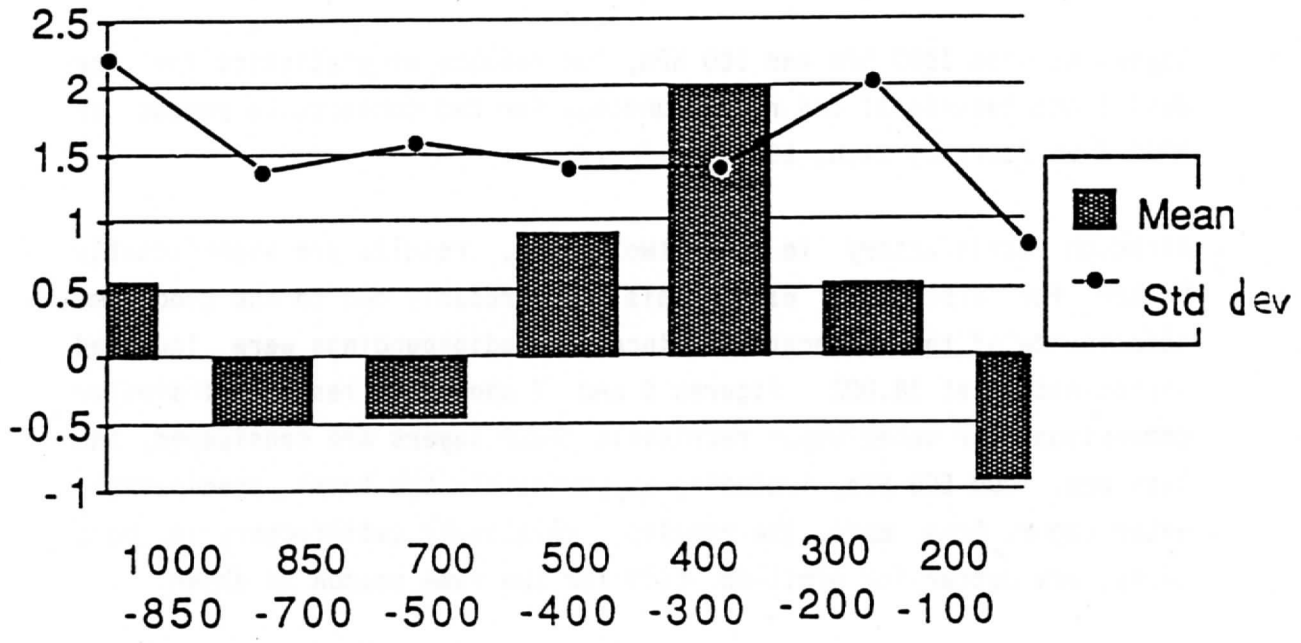

Figure 4 Mean and standard deviation of the differences between 3I retrieved layer temperatures and collocated radiosoundings (about 25 items). NOAA-9 passes 6191. 24 February 1986 at 8.15Z. Radiosoundings at 12.00Z.

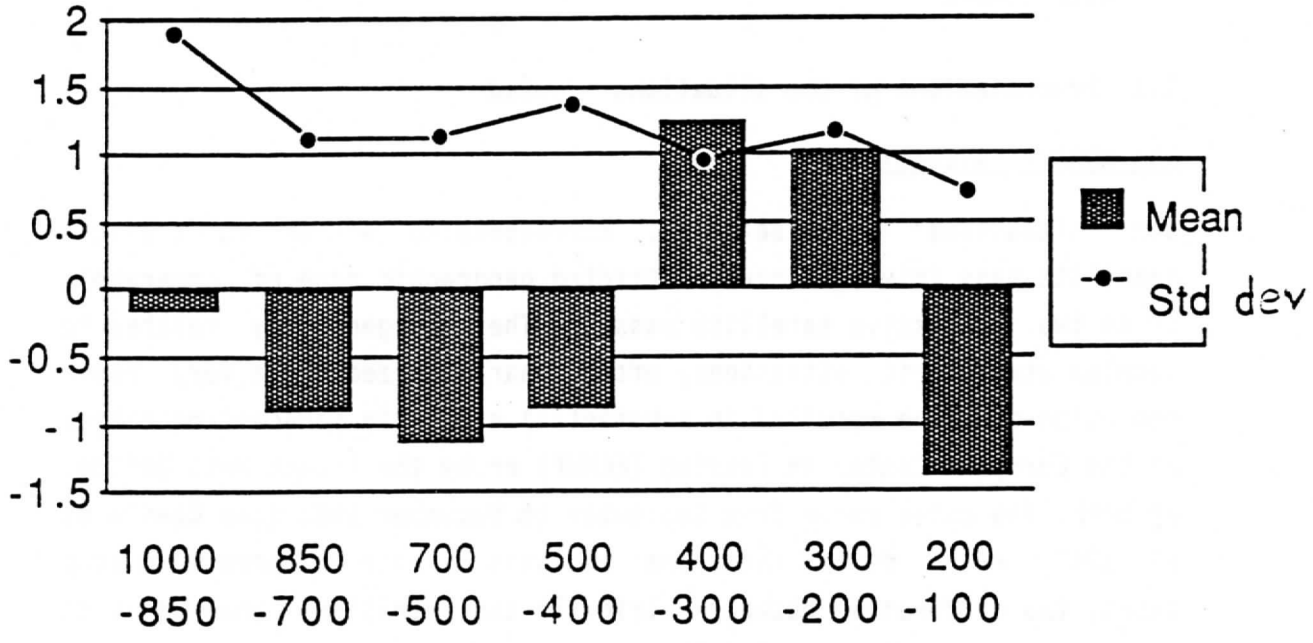

Figure 5 Same as for Figure 4. NOAA-9 pass 6198. 24 February 1986 at 19.32Z. Radiosoundings at 18.00Z.

layers between 1000 hPa and 100 hPa, the results of statistics for the deviations between 3I and radiosoundings for two consecutive passes of NOAA-9 on February 24th, 1986.

Although satisfactory in the two cases, results are significantly better for orbit nb. 6198. This is probably due to the good time coincidence of the collocations since the radiosoundings were launched approximately at 18.00Z. Figures 6 and 7 show the results of similar comparisons for water vapor retrievals. Four layers are considered, the last one, 1000-500 HPa, including approximately the total precipitable water vapor. Once more, the results, relatively satisfactory in both cases, are better for orbit nb. 6198 for the same reason as above.

This work has demonstrated that the 3I system is easily "exportable" and that its use in operational mode is possible, even with limited computer facilities.

5. WATER VAPOR RETRIEVALS FROM NOAA-7 AND NOAA-9 OBSERVATIONS OVER EUROPE

5.1 Presentations of the situations adopted

The NOAA-7 "situations"

Six "situations" were selected, corresponding either to a single satellite pass (giving a more restricted geographic zone of coverage), or to two successive satellite passes. They are generally related to complex atmospheric situations, often characterized by a very rapid evolution and have resulted in substantial errors in forecasting either by the European Center in Reading (ECMWF) or by the French Met. Office, or both. The dates range from September to December 1983 (see Chedin et al, 1987). For a few of them, the analysis is also in error. In such cases, the differences between retrievals and operational analyses must be interpreted having in mind these errors.

A total of nine passes has been studied.

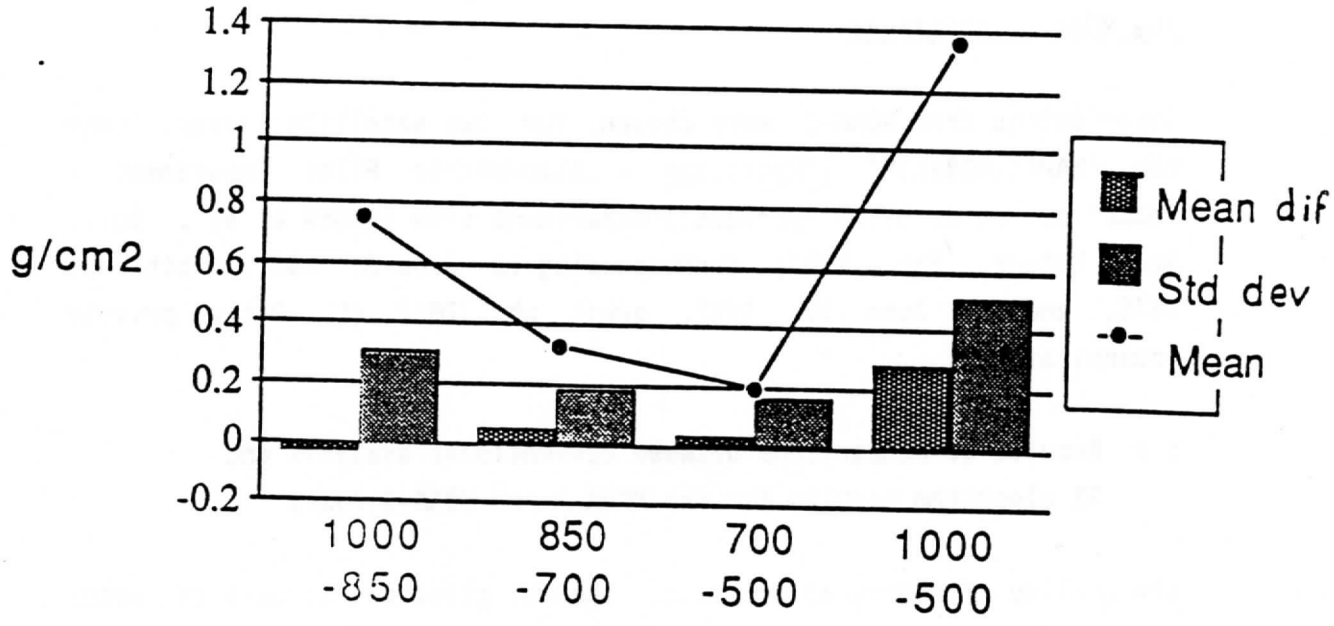

Figure 6 Mean and standard deviations of the differences between 3I retrieved layer precipitable water vapor and collocated radiosoundings (about 15 items). NOAA-9 pass nb. 6191. 24 February 1986 at 8.15Z. Radiosoundings at 12.00Z. Solid line : mean value of the sample.

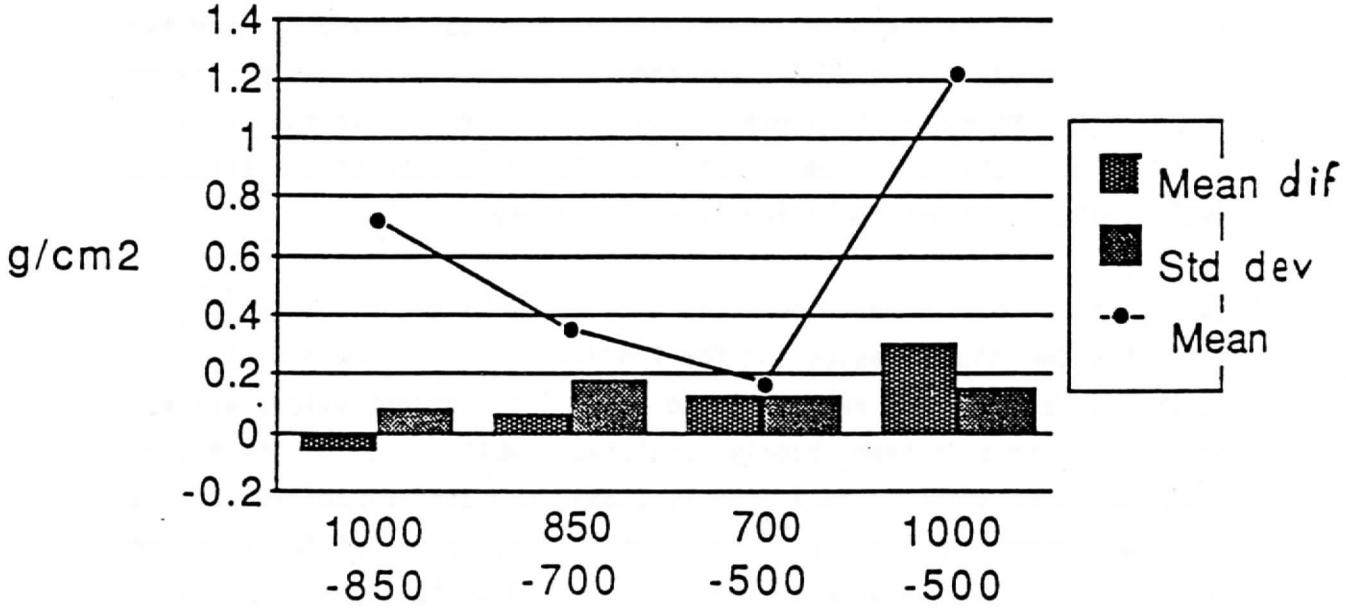

Figure 7 Same as Figure 6. NOAA-9 pass nb. 6198, 24 February 1986 at 19.32Z. Radiosoundings at 18.00Z.

The NOAA-9 situations

Observations from NOAA-9 were chosen, for two satellite passes, over the "HAPEX-MOBILHY" ("Hydrology - Atmospheric Pilot Experiment" - "Modélisation du Bilan Hydrique") experiment site (André et al., Bull. Amer. Meteor. Soc., 1987) corresponding to June 9, 1987, orbit nb. 7676, and to June 19, 1987, orbit nb. 7817 (C. Ottlé, private communication).

5.2 Results of comparisons between conventional analysis and 3I algorithm results for the NOAA-7 and NOAA-9 cases

The quality of retrieved products, thermal structure as well as water vapor related quantities, has been estimated, for the NOAA-7 and NOAA-9 situations mentioned above, through comparisons with ECMWF conventional analyses. Visual comparisons have also been made on the basis of geopotential thickness fields.

A quantitative assessment of the accuracy of the retrieved products has been approached by a statistical analysis of the deviations between the 3I retrievals and the ECMWF thickness fields. The results of this statistical evaluation are reported on Figures 8 and 9 for two representative passes of NOAA-7 and Figures 10 and 11 for two passes of NOAA-9. The parameter considered in these comparisons is the virtual temperature obtained from retrieved layer thicknesses (standard levels). The agreement is basically satisfactory.

Statistics on total water vapor contents ($g.cm^{-2}$) are given on Figure 12 for the two NOAA-9 passes and for 7 NOAA-7 passes. For most of them, rms errors are in the range 25% to 35%. The largest values are for those situations rather poorly analysed (NOAA-7). In one case (not presented in Figure 12), NOAA-7 orbit 11664, the difference between 3I and ECMWF becomes exceptional reaching an rms value of 46 %. Going deeper into the analysis of this result has led us to point out an area for which discrepancies between 3I retrieved and ECMWF analysed total water vapor contents are very large.

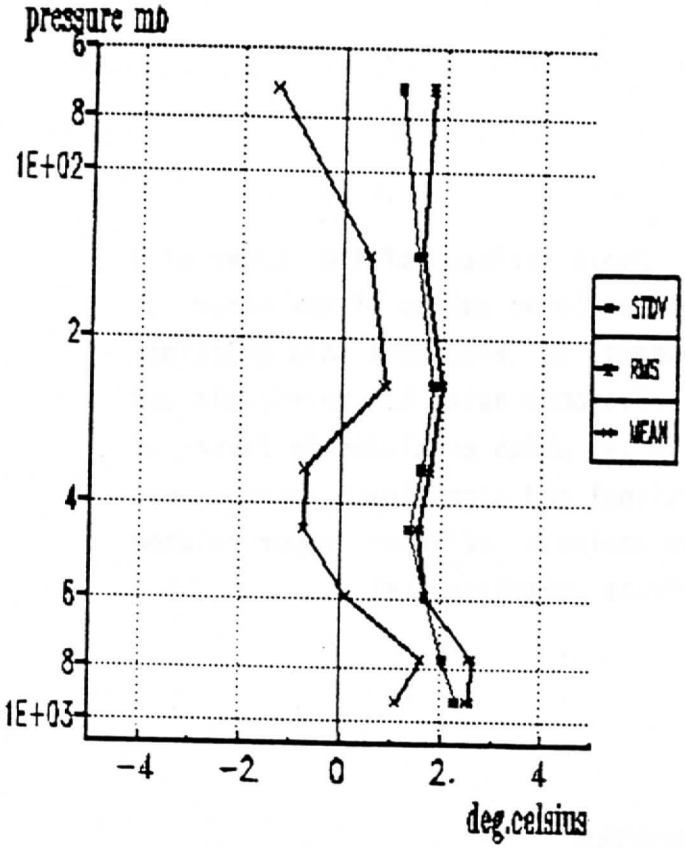

Figure 8 3I retrieval minus ECMWF analysed virtual temperature statistics for NOAA-7, orbit nb. 11664 (27 sept. 1983), 14.35Z).

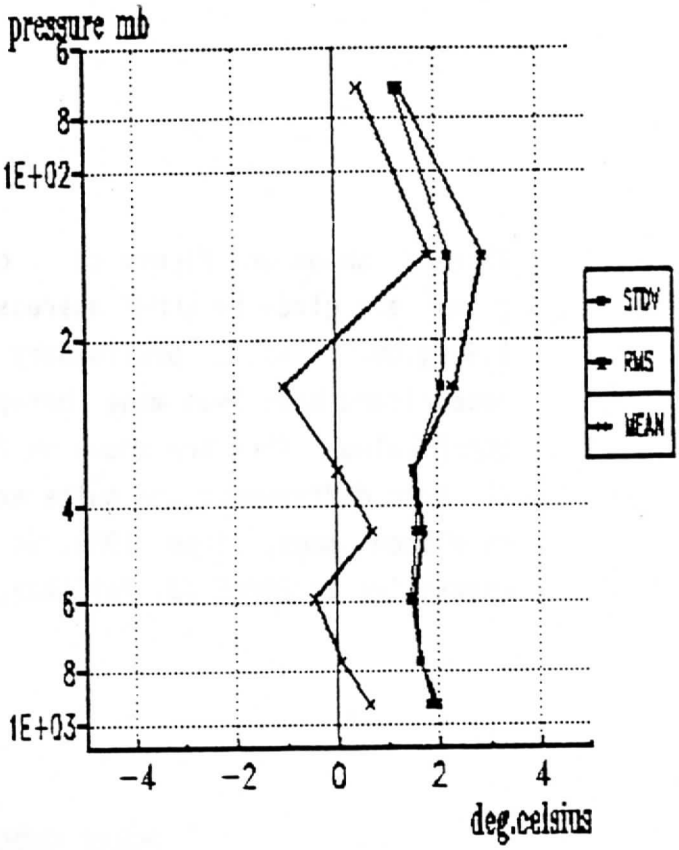

Figure 9 See Figure 8. NOAA-7, orbit nb. 12963 (28 Déc. 1983, 14.17Z).

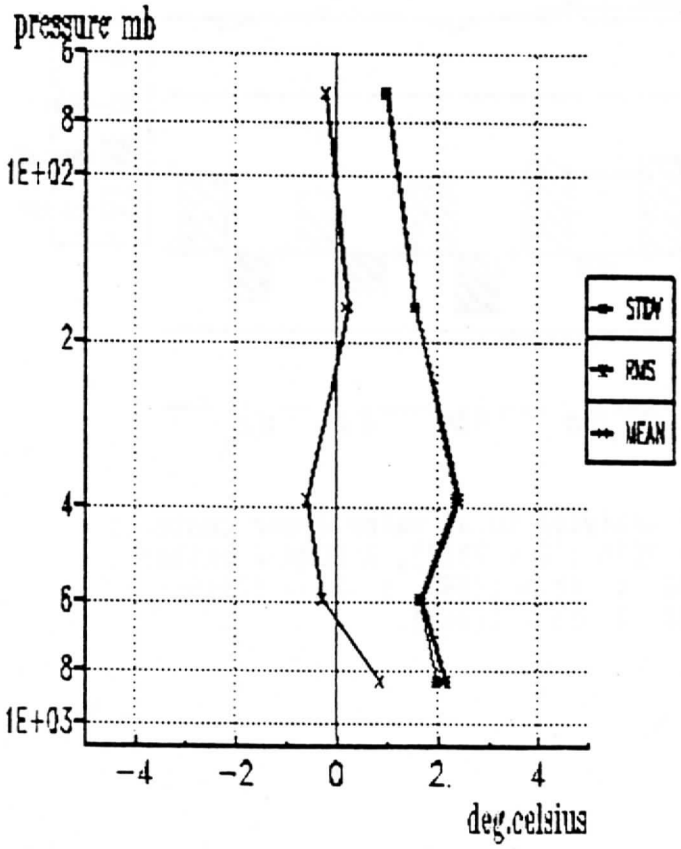

Figure 10 See Figure 8. NOAA-9, orbit nb. 7676 (9 June 1987, 14.02Z).

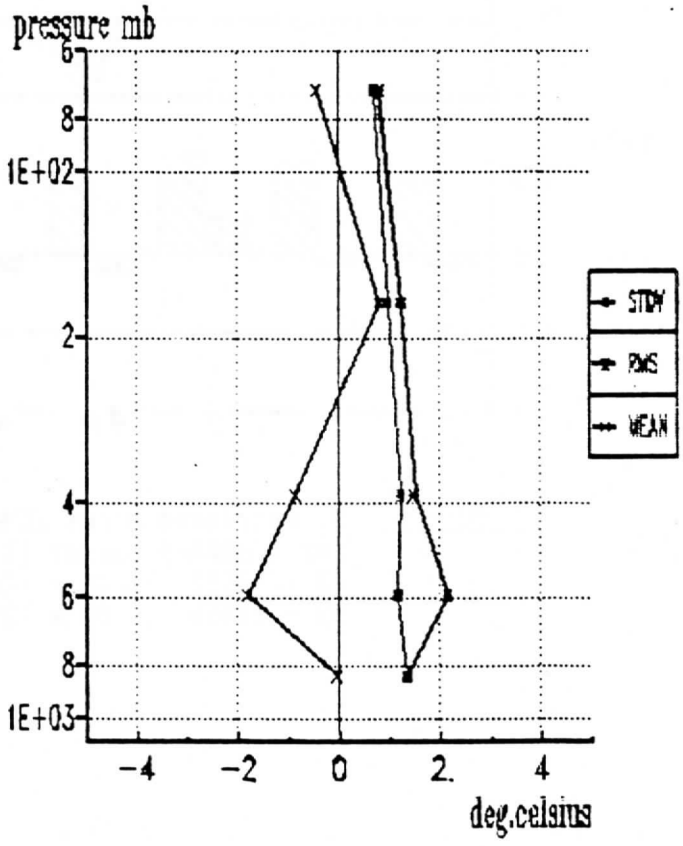

Figure 11 See Figure 8. NOAA-9, orbit nb. 7817 (19 June 1987, 14.39Z).

This is shown on Figure 13 : over Spain, values of the order of 4 $g.cm^{-2}$ are given by ECMWF whereas 3I retrieves values of the order of 1.5 $g.cm^{-2}$. As a preliminary attempt to elucidate this question, comparisons have been made between radiosonde data, 3I retrievals and ECMWF values. They are shown on Figure 14, which concludes in favor of 3I. Such differences are quite exceptional and significant improvements have been made, since 1983, in the analysis of water vapor related quantities at ECMWF (J. Pailleux, private communication).

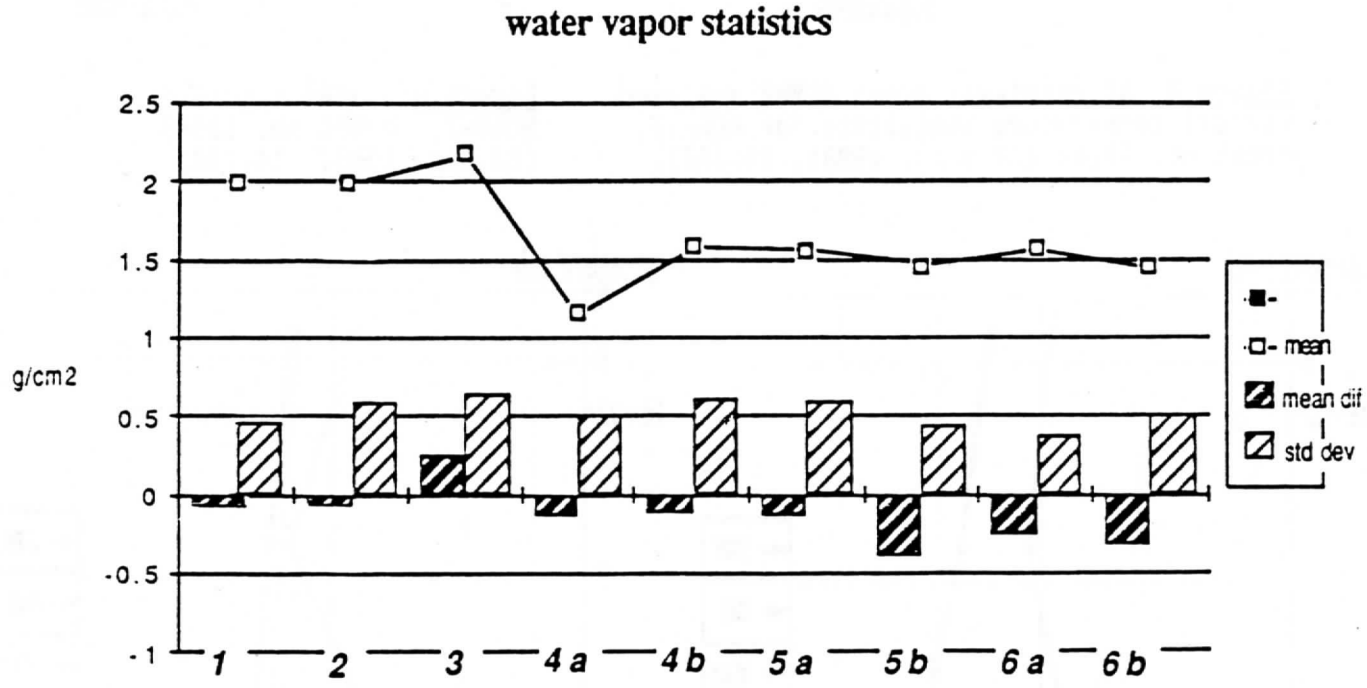

Figure 12 3I retrieved minus ECMWF analysed total water vapor contents for 2 NOAA-9 passes (1 = 7676 ; 2 = 7817), 7 NOAA-7 passes (3 = 12512 ; 4a = 12681 ; 4b = 12682 ; 5a = 12949 ; 5b = 12950 ; 6a = 12963 ; 6b = 12964).

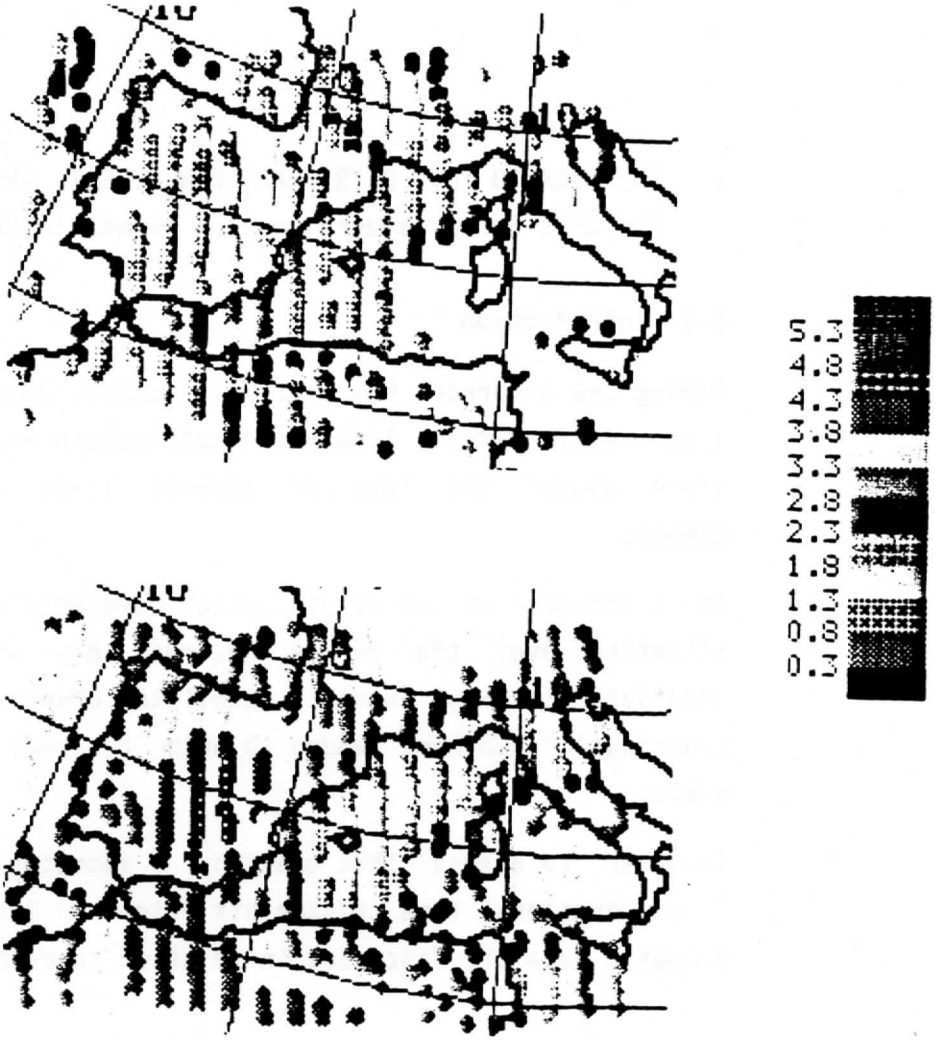

Figure 13

Illustration of an exceptional difference between 3I retrieved (up) and ECMWF analyses (down) of total water vapor content. NOAA-7, 27 sept. 1983, 14.35Z. Radio-soundings for Madrid, La Coruna and Gibraltar favour 3I results.

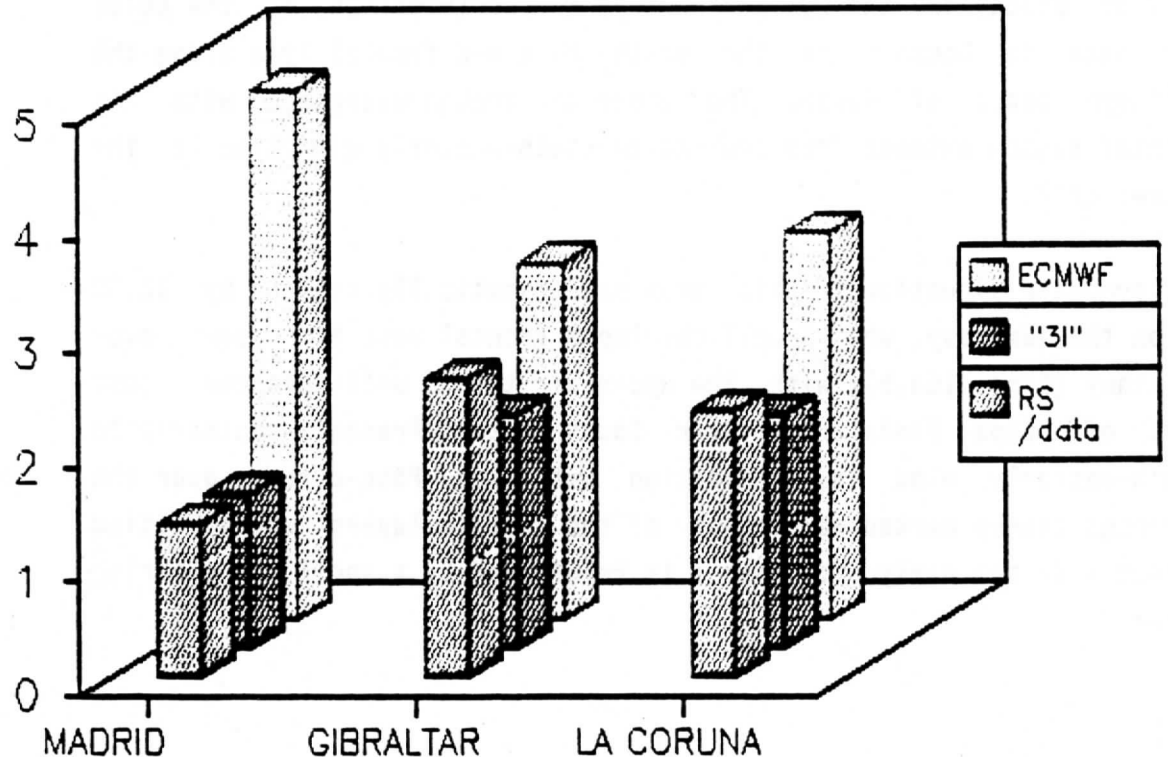

Figure 14

See Fig. 13. Comparison between radiosonde data, 3I retrievals and ECMWF analysis for total water vapor content (g/cm^2).

6. THE NOAA-10 TOVS RETRIEVALS FOR JUNE 7, 1987.
The Whit-Sunday severe weather events in SW France

6.1 Introduction

During the afternoon hours of Whit-Sunday, June 7, 1987, the passage of a very active squall line over Southwestern France with extremely gusty winds caused the loss of several lives and considerable material damage.

The suddenness of the events, which developed out of the meteorological situation over the poorly observed Bay of Biscay, put forward the question, to what extent satellite observations (both imagery and soundings) could have added to help forecast the experienced weather events.

In order to assess this question - admittedly in hindsight and free from operational time constraints - some of the available satellite and synoptic data are discussed in relation to each other.

6.2 Synoptic situation

In the W-SW flow observed at 0.00 UT on the 7th June 1987, over the Gulf of Biscay and the western part of Europe (Figs. 15a,b), the polar air mass is bounded on the south by a W-E frontal line along the northern coast of Spain. The upper-air trough associated with this frontal system extends from Ireland in south-westerly direction to the Azores area.

The synoptic situation in this area has dramatically changed by 12.00 UT on the same day, when a well-developed frontal wave is present over Brittany (Figs. 16a,b), with the upper-air trough well-advanced, just west off Cape Finisterre. Over South-Western France a southerly to south-easterly wind in combination with the Föhn-effect over the Pyrenees causes marked warming-up of the surface layers which heating effect - in the early afternoon - is reinforced by a spell of clearing skies.

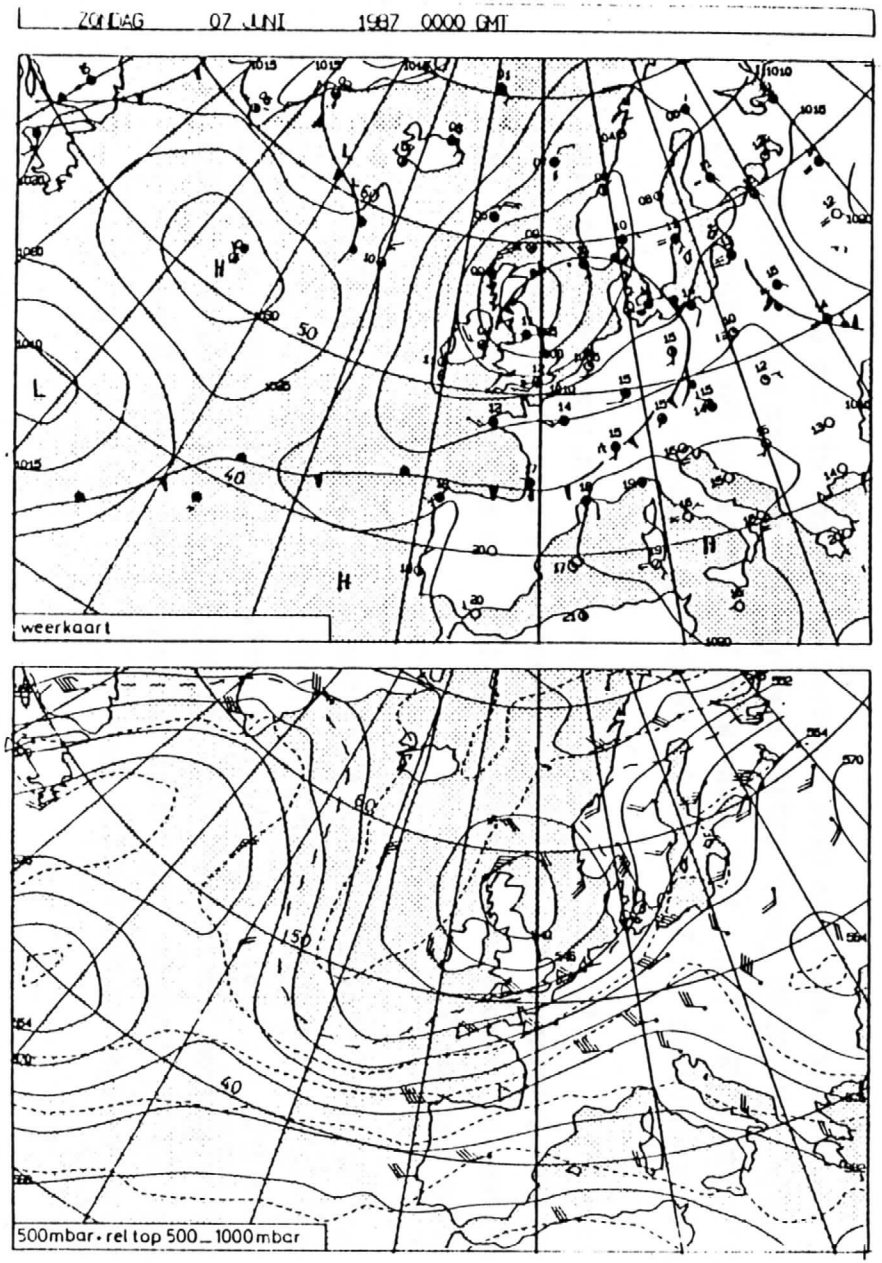

Figure 15 Synoptic analyses for June 7, 1987 at 0.00 UT. (a) : surface map ; (b) : 500 HPa height (full lines) and 1000-500 HPa thicknesses (dashed lines)

[a]

[b]

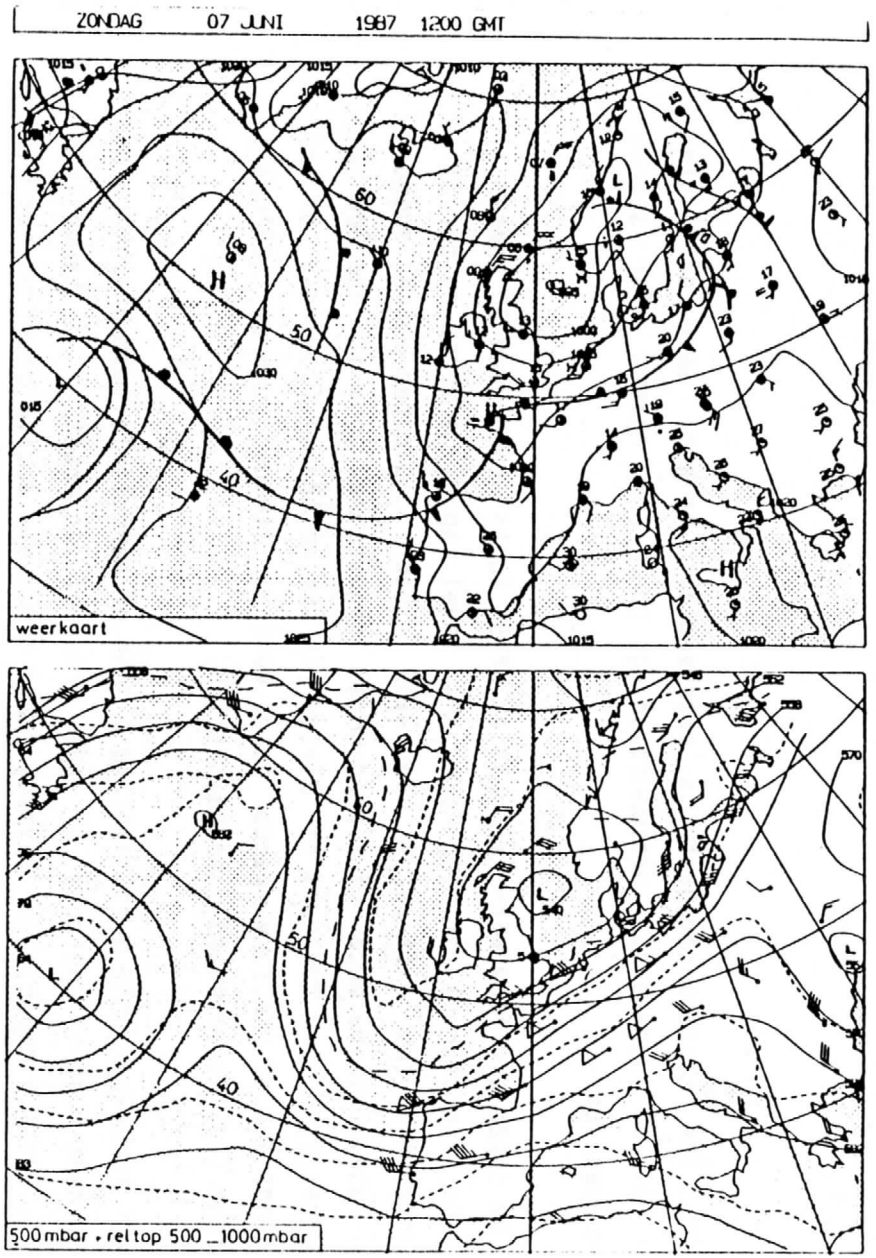

Figure 16 As Fig. 15, for June 7, 1987, at 12.00 UT

Thus the maximum temperatures observed in the area were quite high (26°C at Bordeaux) preconditioning the air column for strong convection.

The upper-air flow with velocities of 50 knots (and even 80 knots at Cape Finisterre) at the 500 hPa level rapidly advects colder air. Moreover, the differences in wind speed, indicated above, suggest already the presence of a pronounced convergence zone at the 500 hPa level also over the Gulf of Biscay. In the northerly flow west of the front and of the convergence zone, cold air (temperature of -25°C are reported) is advected into the region.

All these synoptic data point to a zone of baroclinic instability being present just upstream of the area of interest ; a baroclinic instability capable of causing rapid and very active developments in the 6-hour period to come.

6.3 Satellite data

The available satellite data consist of images of two orbits : from NOAA-9 at 04.40 UT (orbit 12791, see Fig. 17) and from NOAA-10 at 08.55 UT (orbit 3735, Fig. 18), along with TOVS data for the latter orbit, processed using the 3I-system (shown in Figs. 19a-d).

From Fig. 17, it is immediately evident that in the developing wave west of Brittany, the vertical movements are very strong and locally driven by strong convection, resulting in marked variations in the cloud top temperatures.

Further west convective clouds in the cold air behind the front are evidently being organized in a vertical structure (Fig. 17). As can be taken from Fig. 18, where the same vertical cloud structure is barely separated from the frontal wave clouds, this vortex centre is rapidly progressing towards the south-southeast and coming closer to the southern edges of the frontal wave.

From the thermal wind fields (Figs. 19c,d), we conclude that this vortex centre has a complex vertical structure, in that the 1000-850 hPa layer (Fig. 19d) clearly shows two separate cells, whereas the higher layers (850-700 and 700-500 hPa, not shown) display the presence of one cell (near 50N, 13W) only, resulting in a single structure for the whole of the 1000-500 HPa layer (Fig. 19c).

In Fig. 19a, the strong thermal gradient from Brittany to Cape Finisterre and then westward delineates the cold front in the 1000-500 hPa layer, with a marked cold tongue oriented mainly N-S along 13W, with a warmer wedge over the British Iles, indicative of the developing wave.

In the spirit of earlier findings (see Sutcliffe, Q.J.R.M.S., 73, 370-383, 1947 ; Prangsma et al., 1987, and Prangsma, 1988), we have also derived the thermal vorticities for the layers of interest (Figs. 20a-c). From these plots it is readily seen that strong, alternating vorticity gradients exist over a few hundreds of kilometers only, just upstream of our area of interest.

Preliminary estimates - to be followed on by more rigorous analyses - following Sutcliffe's development model suggest strong, alternating cyclonic-anticyclonic-cyclonic developments to have landfall between 4-8 hours after the satellite overpass in the Aquitania coastal region.

6.4 Discussion

As already expressed in the introduction, the following remarks and analyses have been arrived at in hindsight and away from operational time constraints.

The scenario for the weather events in South-West France during the afternoon of June 7, 1987, can - on the basis of the data and analyses presented above - be considered of a rare coincidence of several mutually reinforcing factors :

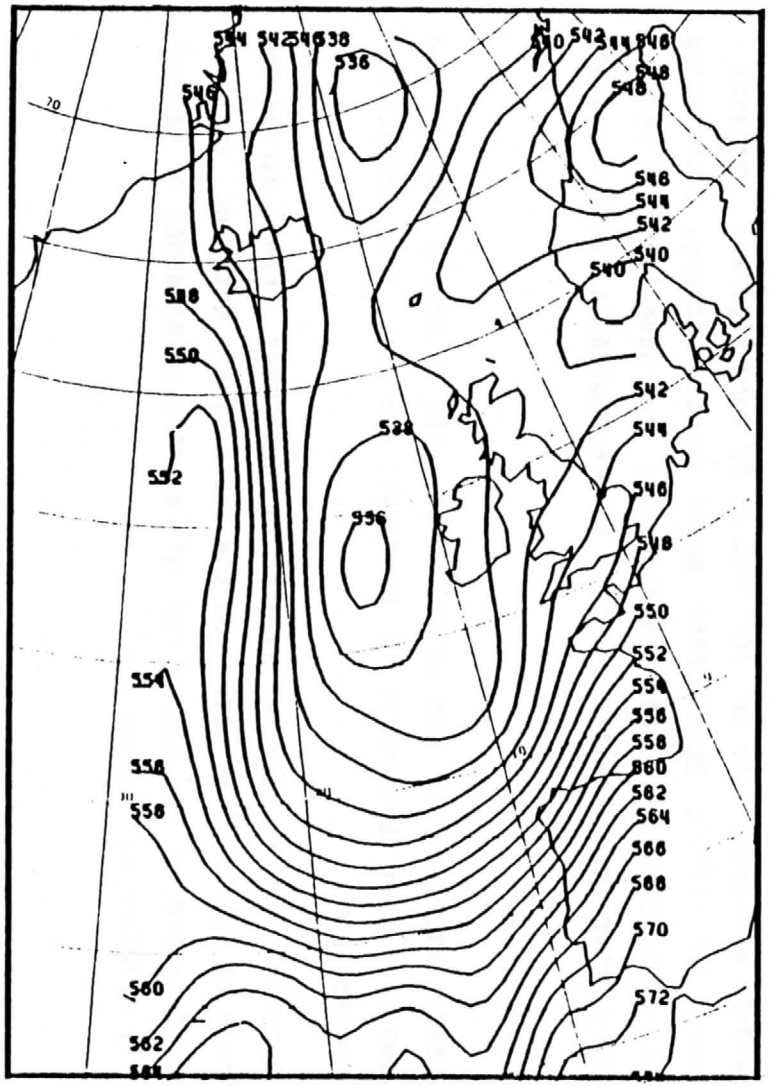

Figure 19a TOVS retrievals for NOAA-10 orbit 3735. 1000-500 HPa thickness.

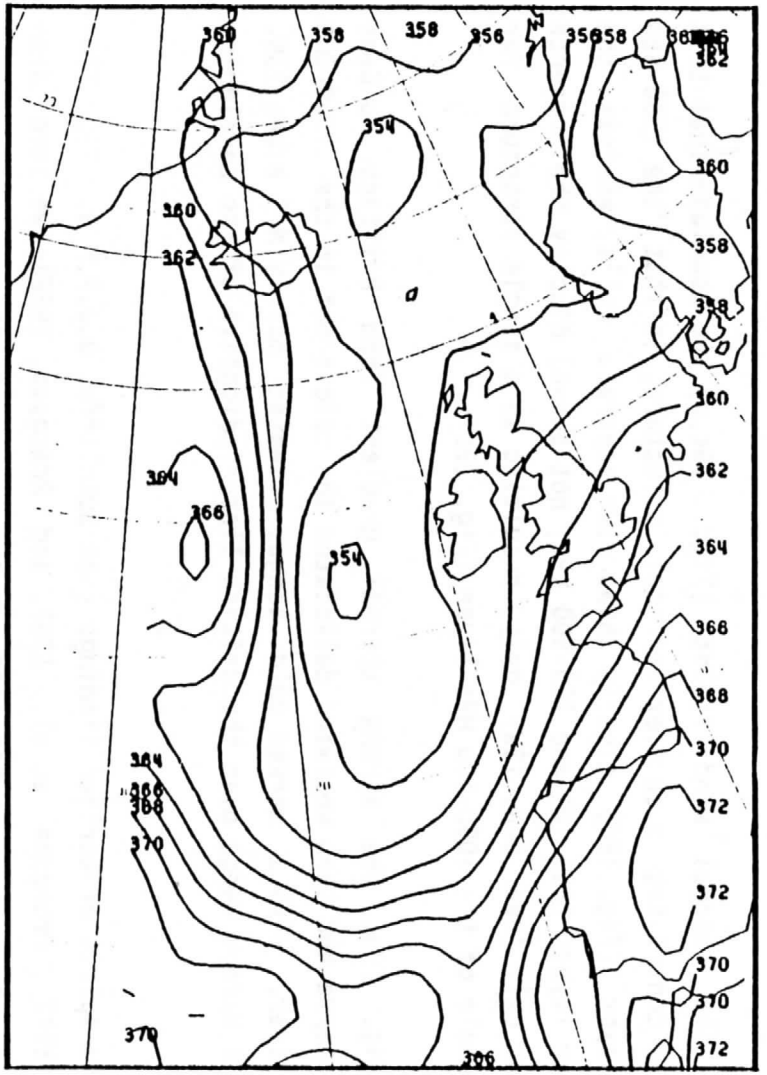

Figure 19b Same as Fig. 19a. 500-300 thickness.

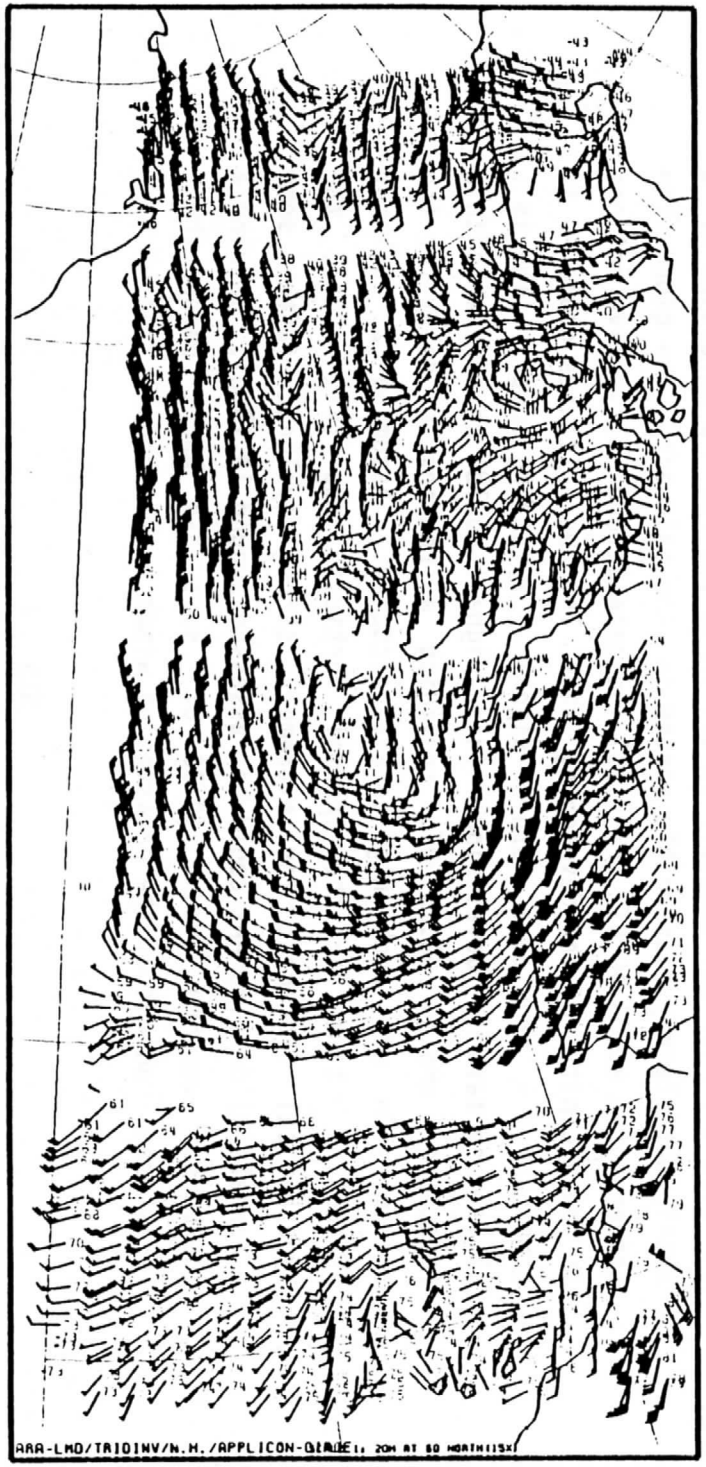

Figure 19c

TOVS retrievals for NOAA-10 orbit 3735, 1000-500 HPa thermal winds.

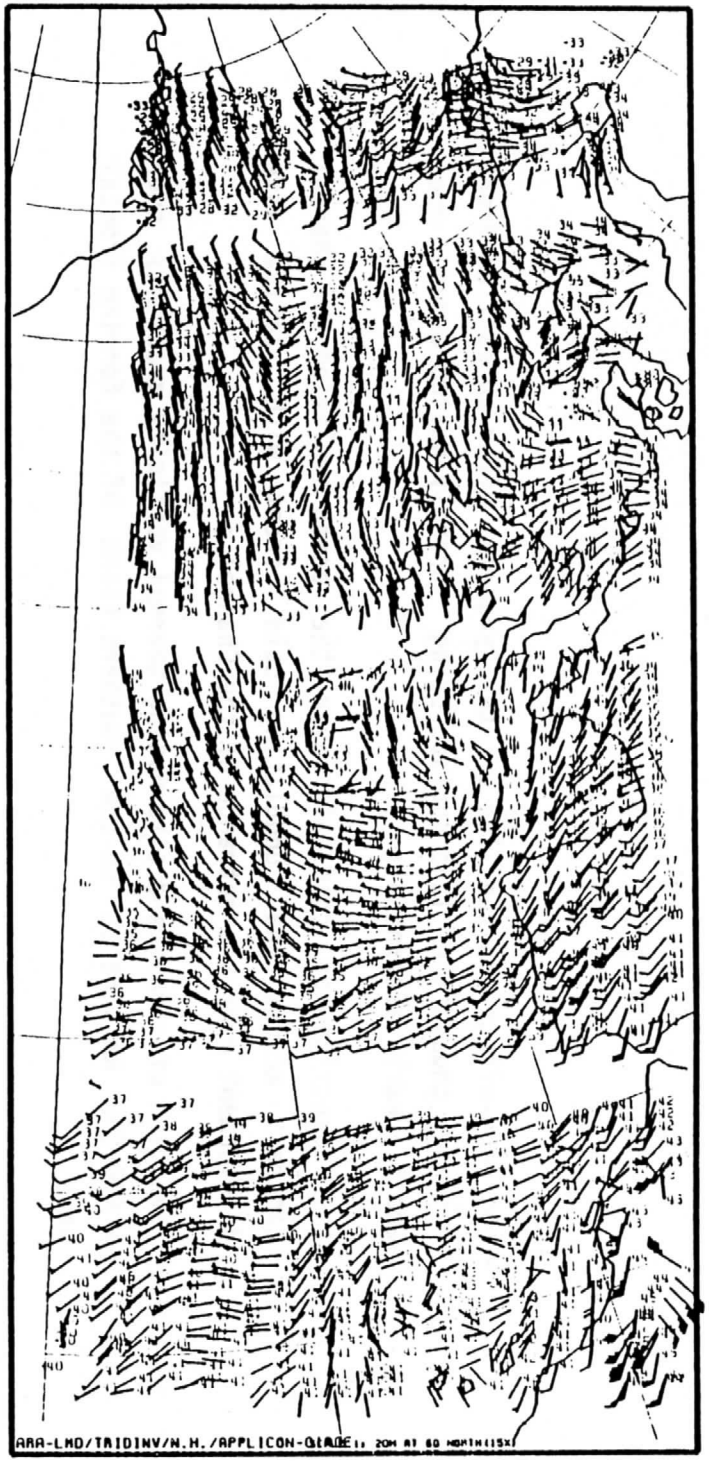

Figure 19d

Same as Fig. 19c, 1000-850 HPa thermal winds.

- the Föhn-effect in the lee of the Pyrenees after an earlier front passing, caused the land surface being strongly heated around noon and the early afternoon ;
- the advection of cold air over the ocean amplified the thermal contrast across the undulating cold front with active wave development over the entrance of the Channel ;
- advection of strong and alternating thermal vorticity gradients over a 400-500 km stretch on the southern flank of the forming frontal wave.

Each of these elements would on its own have led to the formation of thunderstorms in the whole of the coastal region of SW France. It is the combination of the pre-conditioning by the Föhn-effect and the active cold front which led to the formation of a narrow squall line ahead of the cold front, the squall line being rapidly and strongly reinforced by the vorticity advection.

The question could be asked whether or not such developments could have been forecast and by what means.

The detailed imagery (orbit 12791, at 04.40 UT, Fig. 17, and orbit 3735 at 08.55 UT, Fig. 18) combines to delineate the rapid progression of a small, but clearly discernible vortex in the cold air ; the cloud top temperatures at 04.40 UT (Fig. 17) indicate strong convective motions in the vicinity of the developing wave. The two pictures could - in combination - provide a warning signal : a strong squall line is - almost certain - developing. This signal could be available to a forecaster around 09.15 UT, providing a reasonable delay for the transmission of such high-detail pictures. Assuming a one-hour production time for the thermal vorticity map (Fig. 20a), the hypothetical forecast for extremely strong cyclonic (after some alternating) development could be assessed around 10.15 UT, issuing a subsequent warning around 10.30 UT, some 3-4 hours before the - registered - advent of the devastating winds in the squall line.

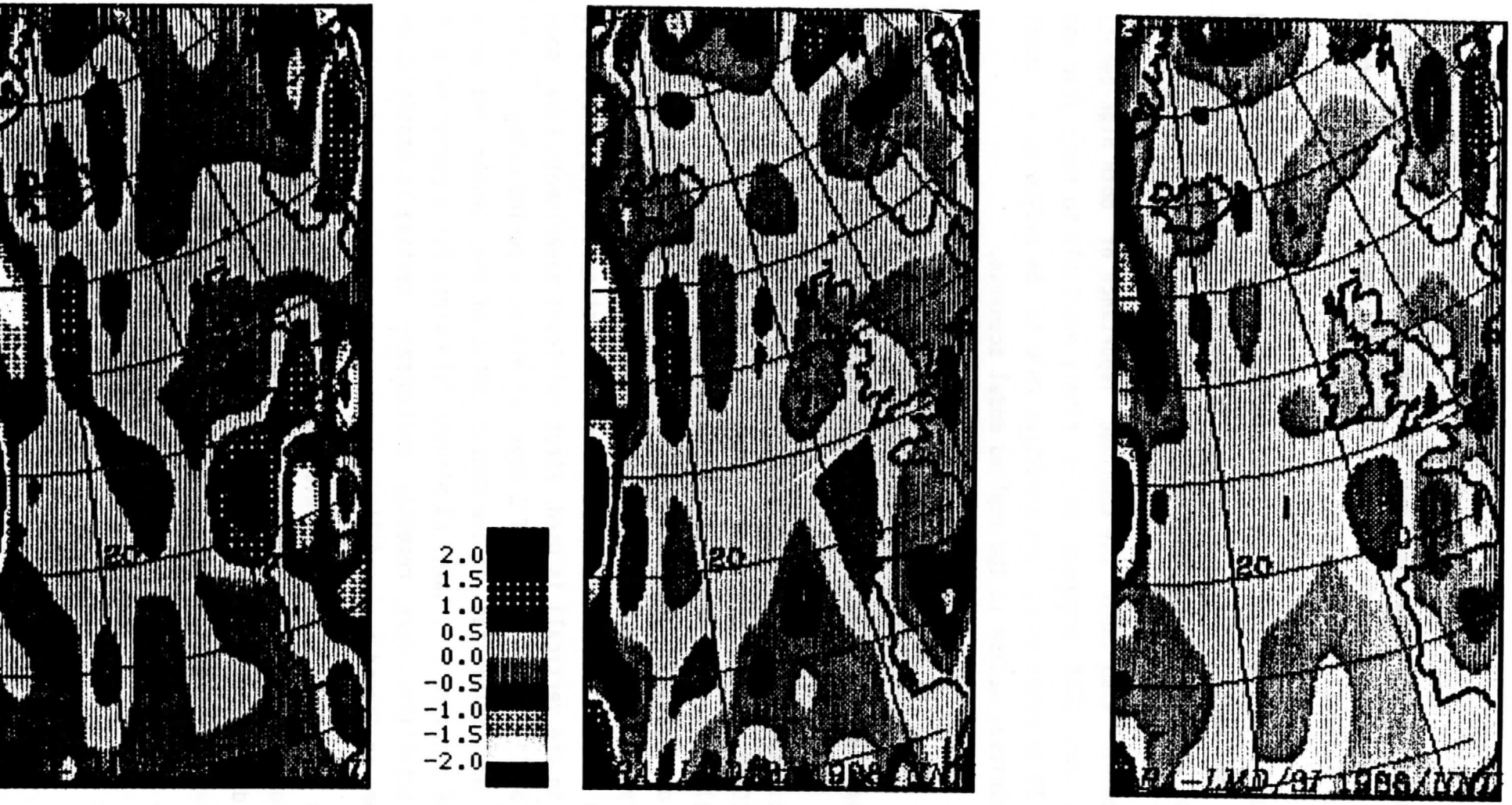

Figure 20 TOVS derived thermal vorticities for NOAA-10. Orbit 3735. (a) : 1000-500 HPa ; (b) : 500-300 HPa ; (c) : 700-500 HPa. (in 10^{-4} s^{-1}).

A suitable limited area model run, assuming a three-hourly update cycle with 2 hours delivery delay, could have confirmed the warning around one hour later (11.15-11.30 UT).

It should be noted that, for such a scenario, a highly sophisticated data - and model - infra-structure is needed. This could however be realized with present day technology.

The scenario also shows the combined importance of both high-detail imagery and TOVS products being timely available to forecaster and model. It moreover shows the essential role to be played by a robust TOVS retrieval method in the implied model scenario.

7. IMPACT OF SATELLITE DATA ON MIDDLE RANGE GLOBAL WEATHER FORECASTING

Since December 1986, the ARA/LMD group participates, in cooperation with ECMWF, in a programme aiming at evaluating the impact of physically retrieved meteorological parameters on the forecast. A one month demonstration period has been chosen from 15 January to 15 February 1987 covered by the two satellites NOAA-9 and NOAA-10. The up-to-date version of the assimilation and forecast system (T106 model, 19 levels in the vertical) is used. First retrieval experiments have been made globally for a period of 5 days within this period using the 3I system. Now implemented on the CRAY-1 XMP48 of the Center, and using only one processor, it takes 23 minutes (CPU time) for a period of 6 h and 2 satellites. Very recently, preliminary testing in assimilation have been performed successfully.

The use of 3I at the ECMWF involves the replacement of the present operational "Satems" (produced by the NOAA-NESDIS in Washington) used in the data assimilation by the corresponding 3I products : thicknesses and relative humidity for the standard layers.

The operational "Satems" received at the ECMWF have a resolution of 250 km, whereas the 3I products have a resolution of about 100 km.

The first assimilation runs have started, over a short period of 18 hours (3 cycles of data assimilation). It has highlighted the spatial coverage of the retrievals, and also the need for a screening aiming at reducing, through quality control, the number of retrievals (about 30,000 per analysis cycle) to a maximum of 15,000 to 20,000 acceptable by the analysis.

Preliminary results show a satisfactory quality, at least as good as the operational NOAA/NESDIS "satems". 3I results seem to be a little less noisy (better standard deviations) and a little more biased, a problem that should be at least partly solved by a better validation of the forward model used.

However, final conclusions have to be drawn on the basis of the impact on the forecast and not on the basis of statistics against radiosondes which cumulate in-situ observation errors and colocation problems.

8. IMPLEMENTATION OF 3I ON VARIOUS COMPUTING SYSTEMS. RECENT DEVELOPMENTS AND SIMPLIFICATIONS

The 3I system is now in use at several places raising the question of an easy maintenance with respect to satellite evolution or replacement.

8.1 The TIGR data set

The 3I system relies upon the TIGR (TOVS Initial Guess Retrieval) data set for both the initialization (pattern recognition) and the inversion (precomputation of brightness temperatures and partial derivatives) process. The validation procedure in use up to recently, was based on the so-called γ-δ procedure : radiances computed from a forward model are adjusted to observations through :

$$I_{obs} = I_{calc} (\tau^{\gamma}) + \delta$$

where γ, in principle close to 1, modifies the computed transmittances and δ represents the instrumental bias. This procedure, quite empirical, has been simplifed due to the good quality of the forward model used resulting in γ values very close to 1 : $|1-\gamma|$ is almost never larger than 0.05 and usually smaller. Since $d\tau$, and not τ, is the quantity governing the retrieval process, the error made by using it, instead of $d(\tau\gamma)$ becomes negligible. Moreover, transparent channels (windows), for which τ itself is used for surface temperature determination, always correspond to γ values equal to 1 as not being affected by this parameter. This is due to the compensation between the surface contribution and the atmospheric contribution to the total radiance.

The interesting consequence is that only δ factors are needed to adjust brightness temperatures to the observation. This correction is made on line within the initialization or inversion routines. A single TIGR data set may then be used whatever the number of platforms to be processed is. The δ values take account of both the γ factors and the slight shifts between the filters from one satellite to the other. The present TIGR data set was computed using NOAA-8 filters. Adaptation to NOAA-10 observations gives rise to reasonably small δ values : the mean of $|\delta|$ for all the channels is close to 0.7 with a standard deviation of 0.6. δ factors are determined, and regularly updated, from satellite and radiosonde matched data using the fast "3R" (Rapid Radiance Recognition) forward model (Flobert et al., 1986). Implemented on the CRAY-1 XMP48 of ECMWF, it takes, as an example, about 2 minutes to compute the brightness temperatures of all the TOVS channels for all the grid points of the forecast model. Its accuracy is equivalent to that of the line-by-line model "4A" (Scott and Chedin, 1981).

The TIGR data set will be soon recreated on the basis of the new NOAA-11 filters, with revised values of CO_2 and N_2O amounts.

8.2 Rejection tests

The 3I system includes tests designed for identifying and rejecting retrievals suspected to be of bad quality. They are based upon comparisons between the observations and the corresponding initialization obtained from TIGR. They have been fully automatized and expressed as functions of channel brightness temperatures standard deviations. These values are obtained from TIGR and take into account the conditions of observation (angle, surface elevation, ...).

A new rejection test has been added, based upon comparisons between initialization and final retrieval and separating the upper and the lower parts of the profiles. A retrieval is rejected if between the two profiles, the distance for the upper part is too different from that for the lower part.

8.3 Exportation of 3I : present status

The 3I system is presently implemented :

- at CMS Lannion (French Met. Office). Bull SPS-9 and IBM-3090,
- at KNMI (Netherlands Met. Office). Micro-Vax II,
- at California Space Institute (Scripps Institution of Oceanography), Micro-Vax I,
- at the European Center for Medium Range Weather Forecasting, CRAY-1 XMP48,
- at Strasbourg University (Scientific Spatial Remote Sensing Group), IBM 4341.

It will be soon implemented at Satellite Meteorologial Center, in Beijing. IBM 4381.

At CNRS-LMD, the 3I system runs on IBM 3090, SIEMENS, VP-200 and CRAY-2. In the latter case, TIGR and associated files are in central memory.

References

Chedin, A., Scott, N.A., Flobert, J.F., Husson, N., Levy, C., Rochard, G., Quere, J., Bellec, B., Siméon, J., "Analyse des champs d'épaisseurs obtenus par la méthode "3I" d'inversion des observations satellitaires de la série Tiros-N". *La Météorologie*, 16, 24-34 (1987).

Chedin, A., Scott, N.A., Wahiche, C. and Moulinier, P., "The improved initialization inversion method : a high resolution physical method for temperature retrievals from the Tiros-N series", *J. Clim. Appl. Meteor.*, 24, 124-143 (1985).

Chedin, A. and Scott, N.A., "Initialization of the radiative transfer equation inversion problem from a pattern recognition type approach", *Advances in Remote Sensing Retrieval Methods*. Academic Press, A. Deepak Ed., 495-515 (1986).

Claud, C., Chedin, A., Scott, N.A. and Gascard, J.C., "Retrieval of meso-scale meteorological parameters for polar latitudes (MIZEX and ARCTEMIZ campaigns). To be submitted to Annales Geophysicae.

FLOBERT, J.F., SCOTT, N.A., CHEDIN, A, 1986, "A fast model for TOVS (Tiros-N Operational Vertical Sounder) radiances computations". 6th Conference on Atmospheric Radiation, May 13-16, 1986, Williamsburg, Va.

Grody, N.C., "Severe storm observations using the Microwave Sounding Unit", *J. Clim. Appl. Meteor.*, 22, 609-625 (1983).

Le Marshall, J.F., 1985, "An intercomparison of temperature and moisture fields from Tiros Operational Vertical Sounder data". The Technical Proceedings of the 2nd International TOVS Study Conference, Igls, Austria. Ed. W.P. Menzel, p. 106-161.

Lindsay, R.W., "MIZEX-84 meteorological atlas and surface data set", Polar Science Center, Univ. of Washington, Seattle, USA (1985).

McMillin, L.M., and Dean, C., "Evaluation of a new operational technique for producing clear radiances", *J. Appl. Meteor.*, 21, 1005-1014 (1982).

Prangsma, G.J., Chedin, A., Scott, N.A., Husson, N., Quere, J., Rochard, G., "Observations of the development of mesoscale systems by operational meteorological satellites". Proc. Symp. Mesoscale Analysis and Forecasting, Vancouver, Canada, ESA SP-282, 117-122 (1987).

Prangsma, G.J., "Mesoscale analysis and the use of TOVS. A case study using 3I results". This volume.

Scott, N.A. and Chedin, A., "A fast line-by-line method for atmospheric absorption computations : the Automatized Atmospheric Absorption Atlas", *J. Appl. Meteor.*, 20, 802-812 (1981).

Wahiche, C., "Contribution au problème de la détermination de paramètres météorologiques et climatologiques à partir des données fournies par les satellites de la série TIROS-N. Impact de la couverture nuageuse", Thèse de 3e Cycle (1984).

Yamamouchi, T. and Seo, Y. "Discrimination of sea ice in the Antarctic, from NOAA-MSU", Proc. 6th Symp. on Polar Meteorology and Glaciology, National Inst. of Polar Research, Tokyo, Japan (1984).

The Technical Proceedings of

The Fourth International TOVS Study Conference

Igls, Austria

March 16-22, 1988

Edited by

W. P. Menzel

Cooperative Institute for Meteorological Satellite Studies
Space Science and Engineering Center
University of Wisconsin
1225 West Dayton Street
Madison, Wisconsin 53706
(608) 262-0544

October 1988